

BLUFF BODY AERODYNAMICS APPLICATION IN CHALLENGING BRIDGE SPAN LENGTH

Yao-Jun Ge*, and Hai-Fan Xiang*

*Department of Bridge Engineering
State Key Laboratory for Disaster Reduction in Civil Engineering
Tongji University, 1239 Siping Road, Shanghai 200092, China
e-mail: yaojunge@mail.tongji.edu.cn

Keywords: Suspension Bridge, Cable-Stayed Bridge, Arch Bridge, Aerodynamic Challenges.

1 INTRODUCTION

With the beginning of the new reform and open policy, 30 years ago, bridge engineering in China has progressed achieving marvelous success, in particular long-span bridge structures. By the completion of Jiangsu Sutong Suspension Bridge in May 2008 and Zhejiang Xihoumen Bridge in 2009, the span lengths of cable-supported bridges are raised up to 1088m for cable-stayed bridges, a new world record with a span jump of 198m, and 1650m for suspension bridges, the second longest in the world, respectively, while China has kept the world record span length for both steel arch bridge, Shanghai Lupu Bridge with the main span of 550m, and concrete arch bridge, Sichuan Wanxian Bridge with the 420m long centre span. There will be fifty-three completed long-span bridges with a main span over 400m in China up to next year, including sixteen suspension bridges, twenty-eight cable-stayed bridges and seven arch bridges [1].

With the rapid increase of bridge span length, bridge structures are becoming more flexible, which requires bluff body aerodynamics studies related to bridge deck flutter instability and vortex induced vibration, as well as stay cable vibration. Aerodynamic stabilization of several suspension bridges recently built in China is firstly introduced, and followed by aerodynamic feasibility study of a 5000m-span suspension bridge. Since cable-stayed bridges intrinsically have quite good aerodynamic stability against flutter oscillation, rain-wind induced vibration and mitigation of long stay cables are discussed as a main concern in long-span cable-stayed bridges. Compared to suspension bridges and cable-stayed bridges, the arch bridge has relatively shorter span, but higher stiffness so that long-span arch bridges may not have wind-induced problem except for Shanghai Lupu Bridge, which suffers vortex-induced vibration and has been controlled by vortex septum.

2 AERODYNAMIC STABILIZATION OF SUSPENSION BRIDGES

The construction of long-span suspension bridges around the world has experienced a considerable development for more than a century. It took about 54 years for the span length of suspension bridges to grow from 483m of Brooklyn Bridge in 1883 to 1,280m of Golden Gate Bridge in 1937, and had an increase by a great factor of about 2.7. Although the further

increase in the next 44 years from Golden Gate Bridge to Verrazano Bridge and to Humber Bridge of 1410m in 1981 was only 10% or by a factor of 1.1, another factor of about 1.4 was realized in Akashi Kaikyo Bridge with a 1,991m main span within 17 years in 1998.

Table 1 lists ten longest-span suspension bridges in the world, including five in China, two in USA, and one in Japan, Denmark and UK, respectively [2]. The information provided in Table 1 covers not only general figures about span, year of completion and location, but also specific concerns related to wind resistance performance, including girder type, wind-induced problem and control measure adopted. The top four suspension bridges in Table 1 all suffered in wind-induced problems in flutter or vortex shedding, and some control measures have been adopted to improve aerodynamic performance, for example, central stabilizer on single box girder for Jiangsu Runyang Bridge, a central slot between twin-box deck for Zhejiang Xihoumen Bridge, both slot and stabilizer in truss girder for Akashi Kaikyo Bridge, and guide vanes on single box girder for Great Belt Bridge.

Span Order	Bridge Name	Main Span	Girder Type	Wind-Induced Problem	Control Measure	Country	Year Built
1	Akashi Kaikyo	1991m	Truss	Flutter	Slot/Stabilizer	Japan	1998
2	Zhejiang Xihoumen	1650m	Box	Flutter	Slot	China	2008
3	Great Belt	1624m	Box	Vortex	Guide vane	Denmark	1998
4	Jiangsu Runyang	1490m	Box	Flutter	Stabilizer	China	2005
5	Humber	1410m	Box	None	None	U.K.	1981
6	Jiangsu Jiangyin	1385m	Box	None	None	China	1999
7	Hong Kong Tsing Ma	1377m	Box	Flutter	Slot	China	1997
8	Verrazano	1298m	Truss	None	None	U.S.A.	1964
9	Golden Gate	1280m	Truss	None	None	U.S.A.	1937
10	Hubei Yangluo	1280m	Box	None	None	China	2007

Table 1: Ten longest span suspension bridges in the world

2.1 Central Stabilizer

Among the top four suspension bridges, Jiangsu Runyang South Bridge completed in 2005 is the second longest suspension bridge in China and the fourth longest in the world. The bridge connects Zhenjiang City and Yangzhou City over Yangtze River at Jiangsu Province in eastern China. The main section of the bridge was designed as a typical three-span suspension bridge with span arrangement of 510m + 1490m + 510m as shown in Fig. 1. The deck cross section is a traditional closed steel box, 36.3m wide and 3m deep, and carries three 3.75m wide traffic lanes in each direction with 3.5m wide shoulders on both sides for emergency use as shown in Fig. 2. The box girder is equipped with classical barriers and sharp fairings intended to improve the aerodynamic streamlining as well as aesthetic quality [3].

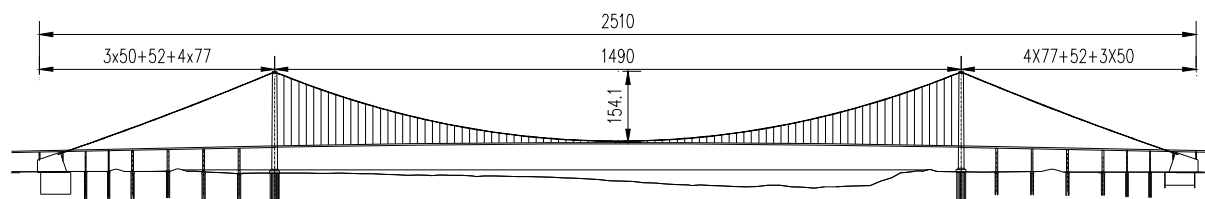


Figure 1: Elevation of Jiangsu Runyang Bridge (Unit: m)

With the structural properties provided in the reference [3], finite element analysis of dynamic characteristics of the prototype bridge was performed, and the symmetrical and antisymmetrical fundamental natural frequencies of lateral, vertical and torsional vibration

modes were calculated and compared with those of the box-girder suspension bridges, including Great Belt Bridge and Zhejiang Xihoumen Bridge in Table 2. The fundamental vertical and lateral bending vibration frequencies of Jiangsu Runyang Bridge are comparable, but the torsional vibration frequencies are relatively lower than those of the other two bridges mainly because of the small depth of the box section.

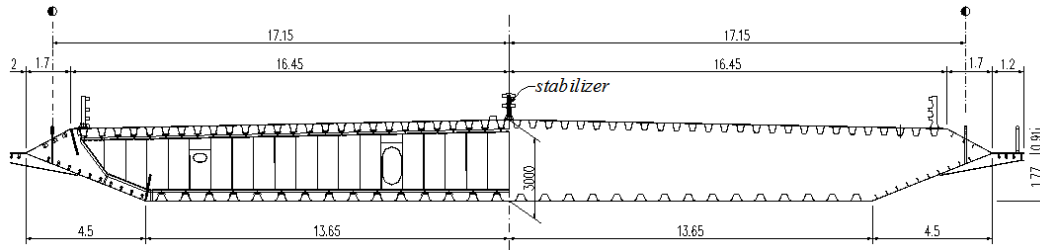


Figure 2: Deck cross-section of Jiangsu Runyang Bridge (Unit: m)

Bridge Name	Span (m)	Lateral Frequency (Hz)		Vertical Frequency (Hz)		Torsional Frequency (Hz)	
		Symmetric	Antisymmetr.	Symmetric	Antisymmetr.	Symmetric	Antisymmetr.
Runyang	1490	0.0489	0.1229	0.1241	0.0884	0.2308	0.2698
Great Belt	1624	0.0521	0.1180	0.0839	0.0998	0.2780	0.3830
Xihoumen	1650	0.0484	0.1086	0.1000	0.0791	0.2323	0.2380

Table 2: Fundamental natural frequencies of three longest box girder suspension bridges

In order to study the aerodynamic stability, a wind tunnel experiment with a 1:70 sectional model was carried out in the TJ (Tongji University) -1 Boundary Layer Wind Tunnel with the working section of 1.8m width, 1.8m height and 15m length. It was found in the first phase of the testing that the original structure could not meet the requirement of flutter speed of 54m/s. Some preventive means had to be considered to stabilize the original structure. With a stabilizer on the central deck as shown in Fig. 2, further sectional model testing was conducted, and the confirmation wind tunnel tests with the full aeroelastic model were also performed in TJ-3 Boundary Layer Wind Tunnel with the working section of 15m width, 2m height, and 14m length. The critical flutter speeds obtained from the sectional model (SM) and full model (FM) wind tunnel tests are collected and compared in Table 3. Both experimental results show good agreement with each other and the central stabilizer of 0.88 m height as shown in Fig. 3 can raise the critical flutter speed over the required value [3].



Figure 3: Central stabilizer mounted on the deck of Jiangsu Runyang Bridge

Box Girder Configuration	Critical flutter speed (m/s)				Required (m/s)
	SM at 0°	FM at 0°	SM at +3°	FM at +3°	
Original box girder	64.4	64.3	50.8	52.5	54
Box girder with a 0.65m stabilizer		69.5	58.1	53.8	54
Box girder with a 0.88m stabilizer		72.1	64.9	55.1	54
Box girder with a 1.1m stabilizer		>75	67.4	56.4	54

Table 3: Critical flutter speeds of Jiangsu Runyang Bridge

2.2 Twin Box Girder

Zhejiang Xihoumen Bridge will become the longest suspension bridge in China and the second longest in the world just behind Akashi Kaikyo Bridge. This bridge is part of the Zhoushan Island-Mainland Connection Project linking two islands, namely Jintang and Cezi in Zhejiang Province. It crosses the Xihoumen channel, one of the most important national deep waterway. The bridge route is selected at the shortest distance of the Xihoumen Strait between Jintang Island and Cezi Island, about 2200m away, with a small island near Cezi, Tiger Island, which can be used to support a pylon for a cable-supported bridge. If one pylon of a three-span suspension bridge sets on Tiger Island, the other one may be placed at the inclined reef of Jintang Island. The location of the pylon foundation on Jintang was compared with different span lengths, for example, above the water level with a minimum span of 1650m, 20m under the water surface with a 1520m span, 35m under the water with a 1310m span, and so on. In order to avoid constructing deep-water foundation, the Xihoumen Bridge is finally designed as a two-span continuous suspension bridge with the main span of 1650m, as shown in Fig. 4 [4].

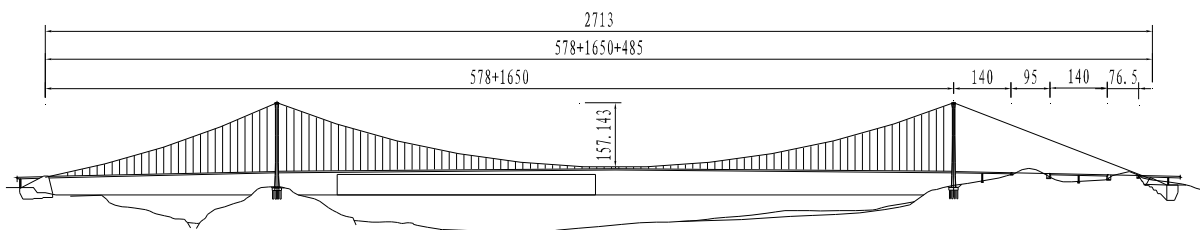


Figure 4: Elevation of Zhejiang Xihoumen Bridge (Unit: m)

Deck Box Girder Configuration	Critical flutter speed (m/s)				Required (m/s)
	-3°	0°	+3°	Minimum	
Single box girder	50.7	46.2	48.7	46.2	78.4
Single box with a 1.2m stabilizer	>89.3	>89.3	37.7	37.7	78.4
Single box with a 1.7m stabilizer	88.0	>89.3	43.4	43.4	78.4
Single box with a 2.2m stabilizer	>89.3	>89.3	88.0	88.0	78.4
Twin box with a slot of 6m	88.4	>89.3	>89.3	88.4	78.4
Twin boxes with a slot of 10.6m	>89.3	>89.3	>89.3	>89.3	78.4

Table 4: Critical flutter speeds of Zhejiang Xihoumen Bridge

Based on the experience gained from the 1490 m Runyang Bridge with flutter speed of 51 m/s and the 1624 m Great Belt Bridge with 65 m/s flutter speed, the span length of 1650 m may cause problems of aerodynamic instability for suspension bridges, even with the stricter stability requirement of 78.4 m/s in Xihoumen Bridge. Four alternative configurations of box girders were proposed and were investigated through sectional model wind tunnel tests. Apart from the traditional single box, the other three deck sections, including the single box with a central stabilizer of 2.2m (Fig. 5a) and the twin box decks with a central slot of 6 m (Fig. 5b)

or 10.6 m (Fig. 5c), can satisfy the flutter stability requirement shown in Table 4, and the 6 m slotted twin-box girder was adopted, which was further modified to the final configuration as shown in Fig. 5d [5].

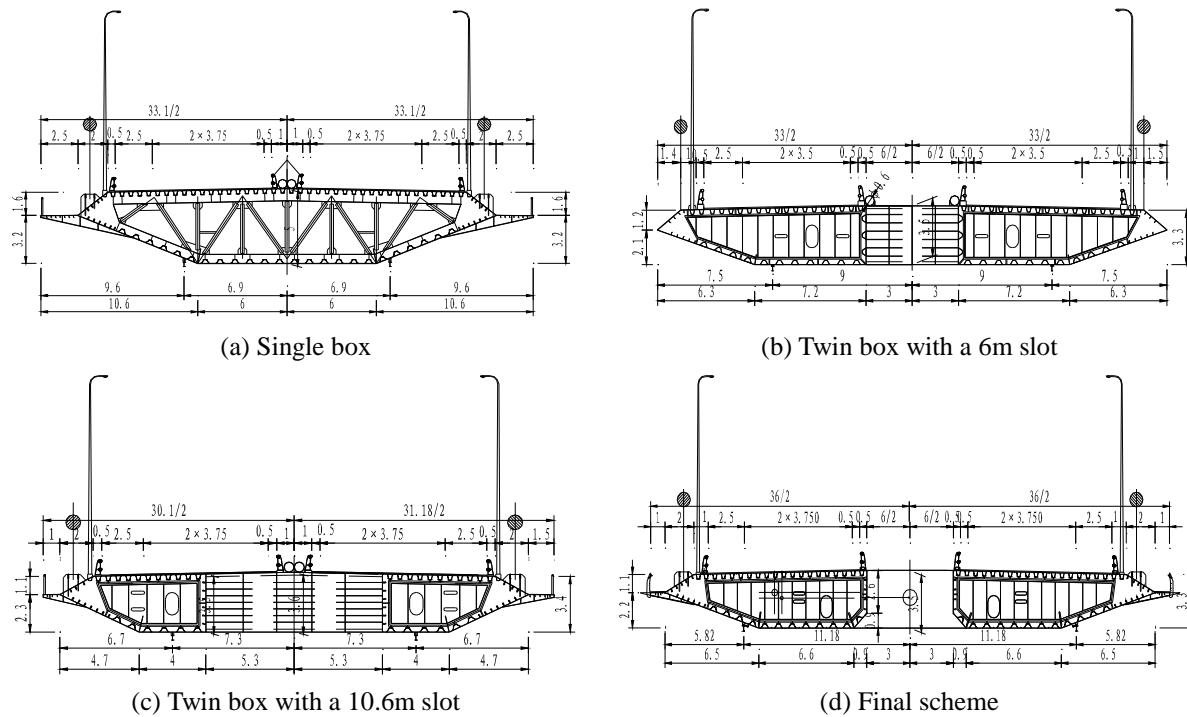


Figure 5: Proposed box girder sections for Zhejiang Xihoumen Bridge (Unit: m)

2.3 Stabilization for Super-Long Span

As a long-time dream and an engineering challenge, the technology of bridging larger obstacles has entered into a new era of crossing wider sea straits, for example, Messina Strait in Italy, Qiongzhou Strait in China, Tsugaru Strait in Japan, and Gibraltar Strait linking the European and African Continents. One of the most interesting challenges has been identified as bridge span length limitation, in particular the span limits of suspension bridges as a bridge type with potential longest span. The dominant concerns of super long-span bridges to bridge designers are basically technological feasibility and aerodynamic considerations. With the emphasis on aerodynamic stabilization for longer span length, a typical three-span suspension bridge with a 5,000m central span and two 1,600m side spans is considered as the limitation of span length as shown in Fig. 6.

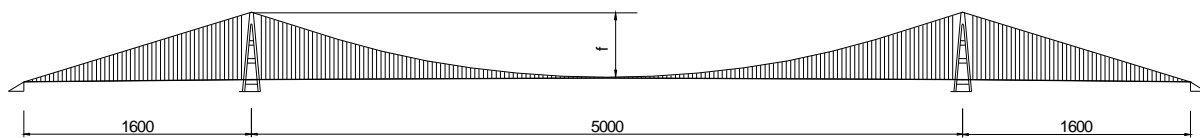


Figure 6: Elevation of the 5,000m long suspension bridge (Unit: m)

In order to push up the aerodynamic stability limit, two kinds of generic deck sections, namely a widely slotted deck (WS) without any stabilizers (Fig. 7a) and a narrowly slotted deck with vertical and horizontal stabilizers (NS) (Fig. 7b), were investigated. The WS cross

section has a total deck width of 80m and four main cables for a 5,000m-span suspension bridge while the NS provides a narrower deck solution of 50m and two main cables [6][7].

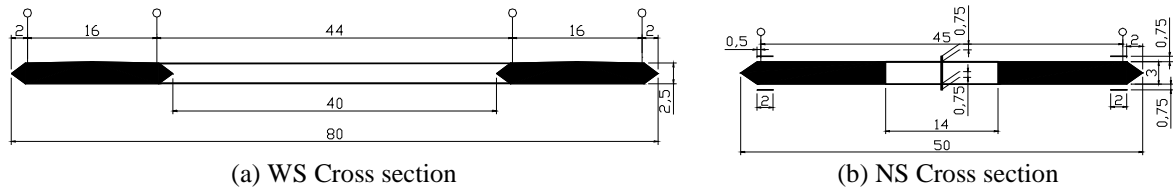


Figure 7: Geometry of deck sections of WS and NS (Unit: m)

Having performed a dynamic finite-element analysis based on the structural parameters listed in Table 5, the fundamental natural frequencies of the structures have been calculated for all four ratios n of cable sag to span and the two deck configurations in Table 6. The fundamental lateral bending frequencies vary about 16% for the WS section and 17% for the NS section from $n = 1/8$ to $n = 1/11$, but almost remain the same between the WS and NS deck configurations. The fundamental vertical bending frequencies are not influenced significantly by both deck configurations and the sag-span ratios. The fundamental torsional frequencies vary differently with the ratio n in the two deck configurations, in which the frequency values go up in the WS section and go down in the NS section with the decrease of the ratio n , but it is interesting to see that the frequency ratio of torsion to vertical bending monotonically decreases with reduction of the ratio n .

Type	Main Cables			Stiffening Girder			
	EA (Nm ²)	m (kg/m)	I_m (kgm ² /m)	EI_y (Nm ²)	GI_d (Nm ²)	m (kg/m)	I_m (kgm ² /m)
WS	0.61~1.12×10 ⁶	2.62~4.82×10 ⁴	2.36~4.33×10 ⁷	4.7×10 ¹¹	2.8×10 ¹¹	24000	2.16×10 ⁷
NS	0.61~1.12×10 ⁶	2.62~4.82×10 ⁴	1.27~2.33×10 ⁷	8.1×10 ¹¹	4.1×10 ¹¹	24000	5.40×10 ⁶

Table 5: Parameters of stiffness and mass of the 5,000m suspension bridge

Ratio	Lateral (Hz)		Vertical (Hz)		Torsional (Hz)		Frequency Ratio	
	WS	NS	WS	NS	WS	NS	WS	NS
$n = 1/8$	0.02199	0.02156	0.05955	0.05936	0.07090	0.09073	1.191	1.528
$n = 1/9$	0.02322	0.02285	0.06126	0.06115	0.07207	0.08928	1.176	1.460
$n = 1/10$	0.02438	0.02406	0.06219	0.06204	0.07268	0.08653	1.168	1.395
$n = 1/11$	0.02548	0.02520	0.06237	0.06219	0.07269	0.08403	1.165	1.351

Table 6: Fundamental natural frequencies of the 5,000m suspension bridge

Ratio	m (×10 ⁴ kg/m)		I_m (×10 ⁷ kgm ² /m)		f_h (Hz)		f_α (Hz)		U_{cr} (m/s)	
	WS	NS	WS	NS	WS	NS	WS	NS	WS	NS
$n = 1/8$	6.01	6.79	5.28	2.37	0.05955	0.05936	0.07090	0.09073	82.9	74.7
$n = 1/9$	6.27	7.43	5.36	3.22	0.06126	0.06115	0.07207	0.08928	88.8	77.4
$n = 1/10$	6.73	8.33	5.92	3.29	0.06219	0.06204	0.07268	0.08653	90.9	78.9
$n = 1/11$	7.66	9.52	6.77	3.62	0.06237	0.06219	0.07269	0.08403	98.9	82.7

Table 7: Critical flutter wind speeds of the 5,000m suspension bridge

With the dynamic characteristics given above and the numerically identified flutter derivatives, the critical wind speeds of the suspension bridges were calculated by multi-mode flutter analysis assuming a structural damping ratio of 0.5%. The results of critical wind speeds together with the generalized mass and mass moment of inertia are summarized in Table 7. For both deck sections the critical wind speed increases with decrease of the ratio n ,

although the frequency ratio of torsion to vertical bending slightly decreases. The most important reason is the considerable increase of the generalized properties in the aerodynamic stability analysis. The minimum critical wind speeds for the WS and NS sections are 82.9 m/s and 74.7 m/s, respectively [8][9].

3 RAIN-WIND INDUCED VIBRATION OF STAY CABLES

Cable-stayed bridges can be traced back to the 18th century, and many early suspension bridges were of hybrid suspension and cable-stayed construction, for example, Brooklyn Bridge in 1883. One of the first modern cable-stayed bridge is a concrete-decked cable-stayed bridge built in 1952 over the Donzere-Mondragon Canal in France, but it had little influence on later development. The steel-decked bridge, Stromsund Bridge in Sweden by Franz Dischinger in 1955, is therefore more often cited as the first modern cable-stayed bridge with a main span of 183m. It took about 31 years for the span length of cable-stayed bridges to increase to 465m in Anacis Bridge in Canada in 1986, but in the last decade of the past century, the span length grew very fast, for example, 520m of Skamsund Bridge in 1991, 602m of Yangpu Bridge in 1993, 856m of Normandy Bridge in 1995 and 890m of Tatara Bridge in 1999. Another big jump with about two hundred meters in span length will be realized in Jiangsu Sutong Bridge with the 1088m length of main span in this year.

Table 8 lists ten longest-span cable-stayed bridges in the world, in which China has contributed eight, and Japan and France have made one contribution each [10]. Except for the Fujian Qingzhou Bridge which experienced aerodynamic instability because of its bluff composite deck, almost all other cable-stayed bridges listed in Table 8 suffered stay cable vibration induced by wind and rain condition, and adopted one or two vibration control measures, including dimples or spiral wires on cable surface, and mechanical dampers at the low ends of cables.

Span Order	Bridge Name	Main Span	Girder Type	Wind-Induced Problem	Control Measure	Country	Year Built
1	Jiangsu Sutong	1088m	Box	Stay cables	Dimples	China	2008
2	Tatara	890m	Box	Stay cables	Dimples	Japan	1999
3	Normandy	856m	Box	Stay cables	Spiral-wires	France	1995
4	3rd Jiangsu Nanjing	648m	Box	Stay cables	Dimples	China	2005
5	2nd Jiangsu Nanjing	628m	Box	Stay cables	Spiral-wires	China	2001
6	Zhejiang Jintang	620m	Box	Stay cables	Spiral-wires	China	2008
7	Hubei Baishazhou	618m	Box	Stay cables	Dimples	China	2000
8	Fujian Qingzhou	605m	Πgirder	Flutter	Guide vane	China	2003
9	Shanghai Yangpu	602m	Πgirder	Stay cables	Damper	China	1993
10	Shanghai Xupu	590m	Box	None	Damper	China	1997

Table 8: Ten longest span cable-stayed bridges in the world

3.1 Dynamic and Aerodynamic Characteristics

The cable-stayed bridge has become the most popular type of long-span bridges in China for the past two decades. In 1993, Shanghai Yangpu Bridge with the main span of 602 m once became the longest span cable-stayed bridge in the world. Although this record was quickly surpassed by Normandy Bridge in 1995 and Tatara Bridge in 1999, China already has 38 long span cable-stayed bridges with main span over 400m including the 1088m Jiangsu Sutong Bridge, and is currently constructing two record-breaking span length cable-stayed bridges, the 1018m Hong Kong Stonecutters Bridge and the 926m Hubei Edong Bridge [9].

There are two great moments in history that the span length of cable-stayed bridges increased with a big jump, 254m from the 602m Yangpu Bridge to the 856m Normandy Bridge in 1995,

and 198m from the 890m Tataru Bridge to 1088m Sutong Bridge in 2008. Is it possible to make further significant increase of span length of cable-stayed bridges? Apart from structural materials and construction technology, among the most important concerns should be dynamic and aerodynamic characteristics.

In order to study dynamic characteristics of a cable-stayed bridge, the finite-element idealization of a cable-stayed bridge is basically carried out with beam elements for longitudinal girders, transverse beams and pylon elements, and cable elements considering geometric stiffness for stay cables, and geometric dimensions and material properties for these elements should be correctly provided. Having performed a dynamic finite-element analysis, the first several natural frequencies of a cable-stayed bridge can be found, and the most important figures are those related to the fundamental vibration frequencies, including lateral bending, vertical bending and torsion modes. The fundamental frequencies of lateral bending, vertical bending and torsion modes of five cable-stayed bridges with a main span over 800m, including Sutong, Stonecutters, Tataru, Normandy and Edong, are collected and compared in Table 9 [9]. Among these five bridges, Tataru Bridge is an exceptional case always with the smallest values of the fundamental frequencies because of the least depth and width of the box girder, but with the largest ratio of the torsional frequency to the vertical frequency. With the unique twin box girder, Stonecutters Bridge has the next smallest fundamental frequencies of lateral and vertical bending modes, but almost the same torsional frequency as Tataru Bridge and Normandy Bridge. As the longest cable-stayed bridge, Sutong Bridge even has higher torsional frequency than those of the other four bridges. It should be concluded that there is not any clear tendency that fundamental frequencies decrease with the increase of span length of cable-stayed bridges.

Bridge Name	Main Span (m)	Lateral Frequency (Hz)	Vertical Frequency (Hz)	Torsional Frequency (Hz)	Frequency Ratio (Tor./Ver.)	Flutter Speed (m/s)	Required Speed (m/s)
Jiangsu Sutong	1088	0.104	0.196	0.565	2.88	88.4	71.6
Stonecutters	1018	0.090	0.184	0.505	2.74	140	79.0
Hubei Edong	926	0.153	0.235	0.548	2.33	81.0	58.6
Tataru	890	0.078	0.139	0.497	3.58	80.0	61.0
Normandy	856	0.151	0.222	0.500	2.25	78.0	58.3

Table 9: Fundamental natural frequencies and critical flutter speeds of five cable-stayed bridges over 800m

The most important aerodynamic characteristic is flutter instability, which can be evaluated by simply comparing critical flutter speed with required wind speed. Critical flutter speed of a bridge can be determined through direct experimental method with sectional model or full aeroelastic model as well as computational method with experimentally identified flutter derivatives, and required wind speed is based on basic design wind speed multiplied by some modification factors, for example, considering deck height, gust speed, longitudinal correlation of wind speed, safety factor of flutter, and so on. Both the critical flutter speeds and the required wind speeds of these five bridges are shown in Table 9. It is very surprising to see that both critical flutter speeds and required wind speeds steadily increase with the increase of main span. Although the reason for this kind of tendency is still under investigation, these long-span cable-stayed bridges with spatial cable planes and steel box girders do not have any problem in aerodynamic instability, and the fact that critical flutter speed is not so sensitive to main span may support to make another jump in span length of cable-stayed bridges in the near future.

3.2 Rain and Wind Induced Vibration of Stay Cables

The most popular wind-resistance problem suffered in these long-span cable-stayed bridges listed in Table 8 is long stay cable aerodynamics under windy and/or rainy weather conditions. Various wind tunnel tests of prototype cable sections were carried out in dry-wind and rain-wind situations, as for example in Sutong Bridge with the outer diameters of 139mm (the most popular cables) and 158mm (the longest cables). As a result, cable vibration is much more severe under the rain-wind condition than under the dry-wind condition for both cable sections shown in Fig. 8, and the maximum amplitudes of these two cables exceed the allowable value of length/1700 [11]. It should be mentioned, however, that the amplitude of rain-wind cable vibration lies on several main factors, and one of the most important factors is spatial cable state, usually described by inclined angle of a cable, α , and yaw angle of wind flow, β . Fig. 9 gives the comparison results, from which the most unfavorable spatial state of a $\phi 139$ cable is under the inclined angle of $\alpha = 30^\circ$ and the yaw angle of $\beta = 35^\circ$, and the wind speed is about 7m/s to 11m/s [12].

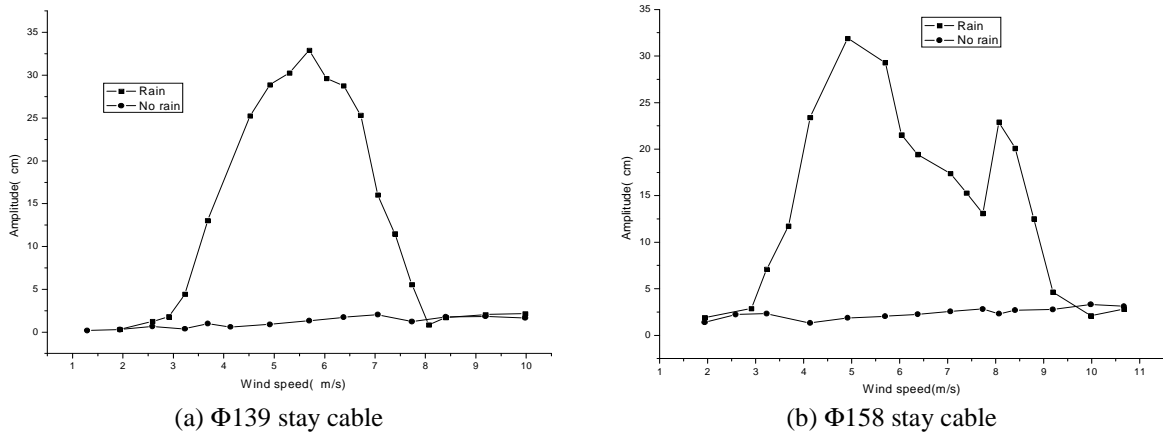


Figure 8: Cable vibration under dry-wind and rain-wind conditions

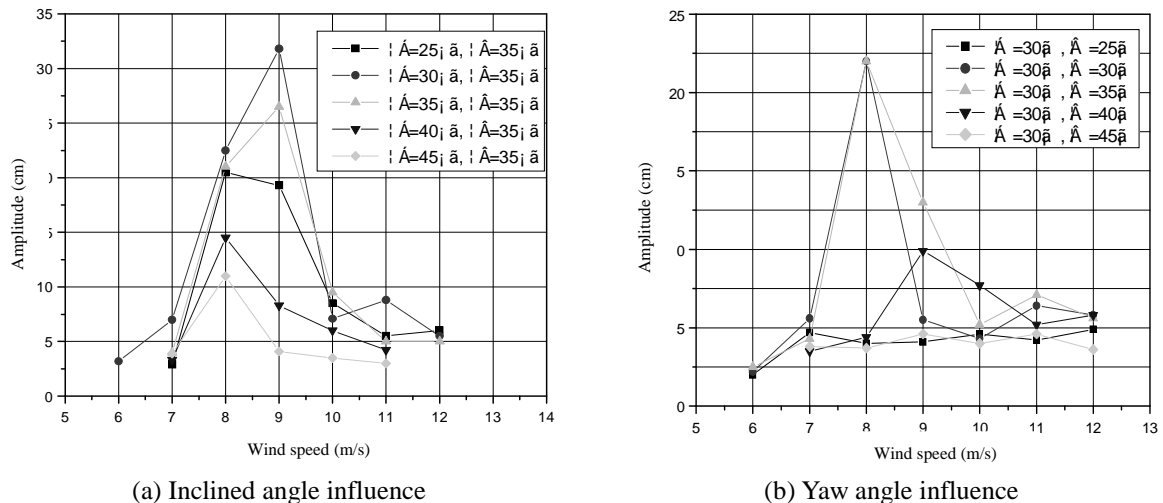


Figure 9: Rain-wind vibration under different spatial states

In order to reduce severe rain-wind induced cable vibration, cable damping has been investigated together with cable vibration frequency. Based on various on-site measurement of cable damping, the average value of cable damping ratio is about 0.15%. Five kinds of

damping ratios and four types of vibration frequencies have been tested, and the main results are presented in Fig. 10. It can be expected that rain-wind induced cable vibration can be effectively controlled with doubling the average damping ratio up to 0.30%, for which numerous damping devices have been produced based on different mechanism, for example, oil pressure, oil viscous shearing, friction, rubber viscosity, magnetic resistance, electrical resistance, and so on [12].

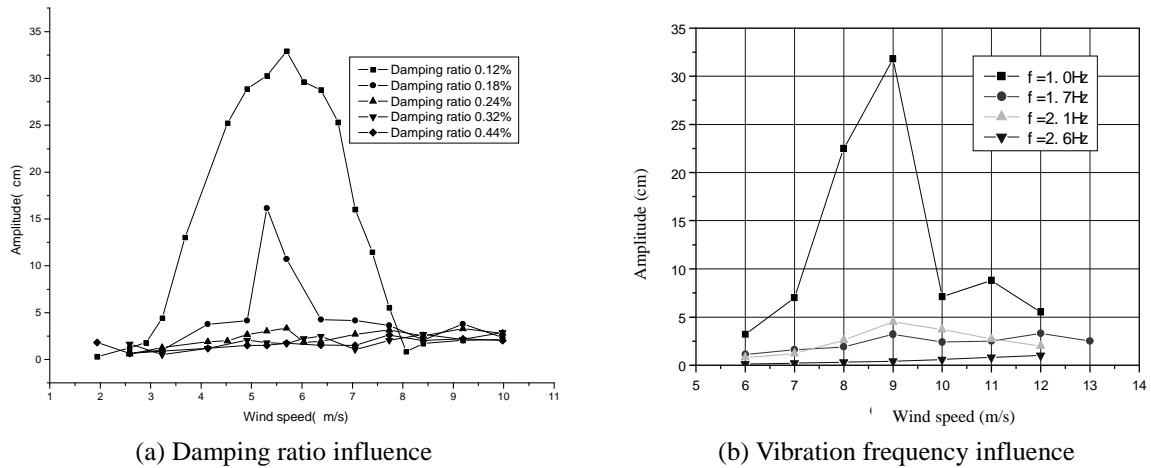


Figure 10: Cable vibration with different damping ratios and frequencies

Another way to ease rain-wind vibration is to prevent cable surface from forming rivulets, which are known as the main effect to generate cable vibration. Two kinds of aerodynamic countermeasures including spiral wires and dimples against rivulets on cable surface were tested and were proven to be sufficient to reduce vibration amplitude to comply with the requirement as shown in Fig. 11. The cable cross ties are also effective to reduce cable vibration not only rain-wind induced but also other vibration, but have been adopted in very few cable-stayed bridges including, for example, Normandy Bridge, one of the ten longest cable-stayed bridges, because of complicated connection with stay cables [12].

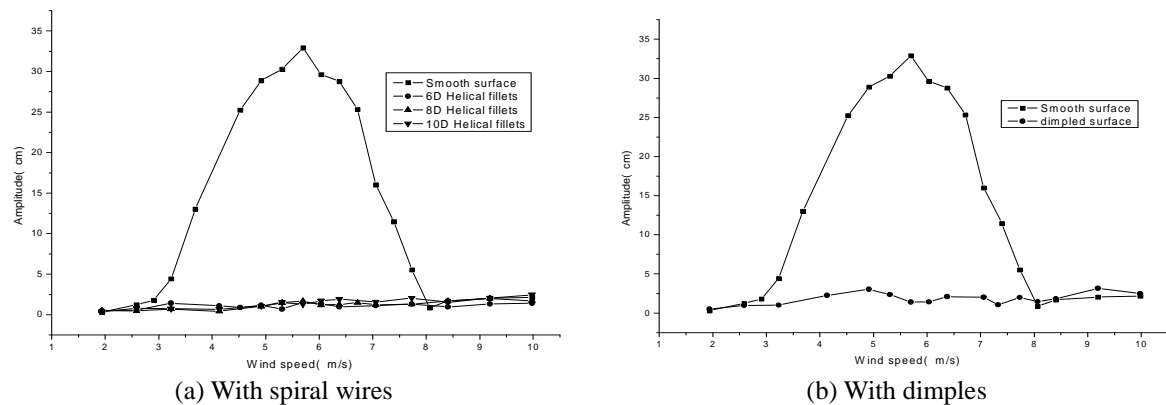


Figure 11: Aerodynamic countermeasures of rain-wind induced cable vibration

4 VORTEX-SHEDDING VIBRATION IN ARCH BRIDGES

Arch bridge is an ancient bridge type originated from stone arches, which were firstly invented around 2500 BC in the Indus Valley Civilization known by the ancient Greeks, but developed most fully for bridges by the ancient Romans, some of whose structures still

survive. China has an ancient history of arch bridge construction for about 2,000 years, and the oldest existing bridge is the Zhaozhou Bridge of 605 AD, which is the world's first wholly-stone open-spandrel segmental arch bridge. In more modern times, stone and brick arches continued to be built by many civil engineers, but different materials, such as cast iron, steel and concrete have been increasingly utilized in the construction of arch bridges. The longest arch bridge of the 19th century is Műngsten Viaduct Bridge with the 170m main span in Germany, which kept the world record until the 310m Hell Gate Bridge built in USA in 1916. In the 1930's, two famous long-span arch bridges were completed, namely the 504m Bayonne Bridge of USA and the 503m Sydney Harbor Bridge of Australia, which had become the longest arches for about 45 years, till the emergence of 518m New River Gorge of USA in 1977. In this new century, China has built several remarkable arch bridges with record-breaking span length, for example, the 420m Sichuan Wanxian Bridge as the longest concrete arch, the 460m Sichuan Wushan Bridge as the longest arch bridge with concrete-filled steel tube arch ribs, the 550m Shanghai Lupu Bridge as the longest steel arch, and the 552m Chongqing Caotianmen Bridge as the new record span length arch to be completed this year. Ten longest-span arch bridges in the world are shown in Table 10 [13], and only one of them, namely Shanghai Lupu Bridge, suffered wind-induced vibration problem, vortex-shedding oscillation due to bluff cross sections of arch ribs.

Span Order	Bridge Name	Main Span	Girder Type	Wind-Induced Problem	Control Measure	Country	Year Built
1	Ch.Q. Caotianmen	552m	Truss	None	None	China	2008
2	Shanghai Lupu	550m	Box	Vortex	Cover plate	China	2003
3	New River Gorge	518m	Truss	None	None	USA	1977
4	Bayonne	504m	Truss	None	None	USA	1931
5	Sydney Harbor	503m	Truss	None	None	Australia	1932
6	Sichuan Wushan	460m	Tube	None	None	China	2005
7	G.D. Xinguang	428m	Truss	None	None	China	2008
8	Sichuan Wanxian	420m	Box	None	None	China	2001
9	Chongqin Caiyuanba	420m	Box	None	None	China	2008
10	4th Hunan Xiantan	400m	Tube	None	None	China	2007

Table 10: Ten longest span arch bridges in the world

4.1 Vortex Shedding Vibration of Arch Ribs

Shanghai Lupu Bridge over Huangpu River is a half-through arch bridge with two side spans of 100m and the central span of 550m, the longest span of arch bridges in the world. The orthotropic steel girder provides six-lane carriageways in the center of the deck and two sightseeing pedestrian ways on both sides, which are supported by arch ribs with several hangers and columns. There are eight horizontal post-tensioning strands in both sides of the girder between the end cross beams to balance the dead load thrusts in the central span arch ribs. The entire steel arch-beam hybrid structure is composed of arch ribs, orthotropic girder, spatial hangers and columns, bracings between two ribs, and horizontal post-tensioning strands as shown in Fig. 11 [14].

The two inclined arch ribs are 100m high from the bottom to the crown, and each has the cross section of a modified rectangular steel box with 5m width and depth of 6m at the crown and 9m at the rib bases as shown in Fig. 12, a configuration for which vortex-induced vibration could occur in vertical and lateral bending modes of arch ribs in the completed bridge structure and during construction, for example, the maximum rib cantilever and the completed arch ribs. Careful investigation in aerodynamic aspects on wind induced oscillation of Lupu Bridge has been conducted based on the feature of the wind environment around the

bridge site in Shanghai in order to ensure aerodynamic stability and safety of the arch ribs and the whole bridge during construction and after completion. It was found from the investigation that the most unfavorable aerodynamic effect is severe vortex-induced vibration (VIV) of arch ribs after completion and during construction. In order to avoid severe VIV, some aerodynamic preventive measures have been investigated, and certain measures should be adopted in this bridge [15].

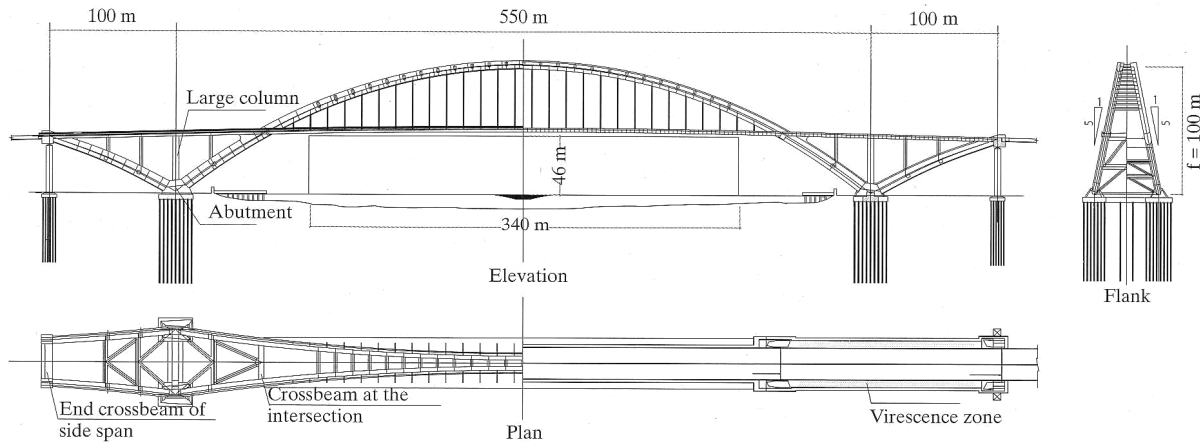


Figure 11: General arrangement of Shanghai Lupu Bridge (Unit: m)

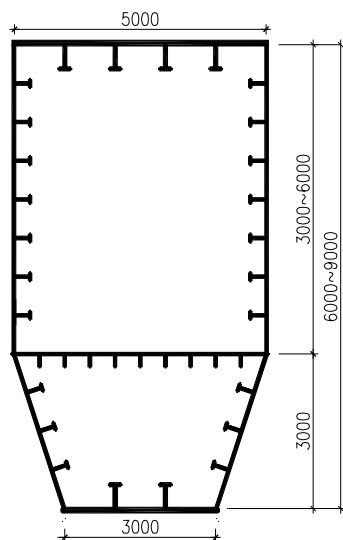


Figure 12: Rib cross section (Unit: mm)

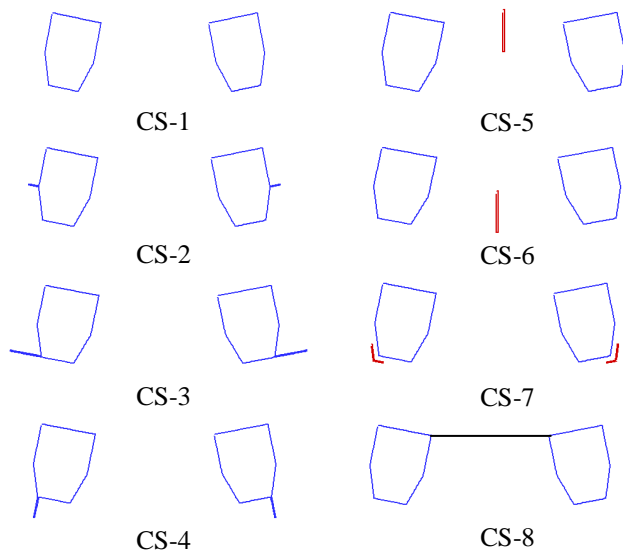


Figure 13: Preventive measures of arch rib against VIV

4.2 Numerical Simulation of Preventive Means

Although bridge aerodynamics is traditionally investigated through physical testing methods or analytical approaches based on experimentally identified parameters, the application of numerical simulation becomes more and more accessible to aerodynamic design of bridge member geometry and checking of structural performance. Numerical simulation based on computational fluid dynamics (CFD) provides alternative possibilities for physical experimentation, for example, wind tunnel testing, which often proves expensive and time-consuming.

The random vortex method code RVM-FLUID [16] developed in Tongji University in 2002 was used to analyze the two-dimensional model of a couple of rib cross sections with the

average depth of 7.5m. It was found that severe VIV happens with the amplitude of $0.028H$ (rib depth) at the Strouhal number (reduced frequency) $S_r = 0.156$. In order to improve resistance to VIV of the bluff cross section of the ribs, several aerodynamic preventive measures as shown in Fig. 13 were numerically tested, and the calculation results including Strouhal numbers and relative amplitudes are listed in Table 11. There are only four effective schemes of preventive measures, including CS-2, CS-6, CS-7 and CS-8, which can reduce amplitude of VIV to some extent. Among these four schemes, the best solution is the scheme of the full cover plate (CS-8), which can reduce the amplitude to only about 40% of that in the original configuration [17].

Case	Rib Configuration	Strouhal	z_{max}/H^*	Reduced
CS-1	Original structure	0.156	0.028	
CS-2	2m middle plates	0.220	0.025	11%
CS-3	2m bottom plates (H)	0.137	0.034	
CS-4	2m bottom plates (V)	0.137	0.032	
CS-5	4m top stabilizer	0.137	0.032	
CS-6	4m bottom stabilizer	0.156	0.017	39%
CS-7	4m corner deflectors	0.175	0.023	18%
CS-8	Full cover plate	0.156	0.011	61%

* z_{max} is the maximum VIV amplitude, and H is the rib depth.

Table 11: Strouhal number and relative amplitudes

4.3 Wind Tunnel Testing Confirmation

The aeroelastic model for confirming effectiveness of the full cover plate was designed with a linear scale of 1:100 of the prototype structure with the entire model simulated in sufficient detail including anti-collision walls and other deck details. Apart from Reynolds number, the similarities of the other dimensionless quantities were carefully adjusted. The full aeroelastic model of Lupu Bridge was designed and constructed for the structure configurations corresponding to three construction stages, the maximum rib cantilever (MRC), the completed arch rib (CAR), and the completed bridge structure (CBS). The wind tunnel experiments of VIV with aeroelastic models were carried out in the TJ-3 Boundary Layer Wind Tunnel as shown in Fig. 14 [17].



Figure 14: Aerodynamic model of Shanghai Lupu Bridge

Several wind tunnel testing cases were conducted for three bridge configurations with or without preventive measures under different angles of attack and different yaw angles. The measured data include the displacements of arch ribs and stiffening girder at the mid-span ($L/2$) and the quarter span ($L/4$) of the centre span, and the displacements at the top of one temporary tower. Due to the bluff feature of the arch rib sections, significant VIV oscillation was observed in vertical and lateral bending modes during testing. Two types of aerodynamic preventive measures were experimentally investigated, including the full cover plate between two arch ribs (scheme A) and the partial cover plate with 30% air vent (scheme B). The main experimental results including the maximum displacements of vertical and lateral VIV of the arch ribs at the mid span ($L/2$) and the quarter span ($L/4$) are listed in Table 12. It can be concluded that scheme A or B effectively makes it possible to reduce VIV amplitudes [15].

Erection Stage	Attack Angle	Control Measures	Speed (m/s)	Frequency (Hz)		L/2 Amplitude (m)		L/4 Amplitude (m)	
				Vertical	Lateral	Vertical	Lateral	Vertical	Lateral
Maximum Rib Cantilever (MRC)	0°	Original	16.3	0.393	0.408	0.813	0.308	0.216	
			26.3	0.393	0.408	0.656	0.272	0.176	
		Scheme A	17.5	0.393	0.408	0.590	0.237	0.166	
			25.0	0.393	0.408	0.333	0.144	0.100	
Scheme B	16.3	0.393	0.408	0.249	0.115	0.069			
	42.5	0.883	0.408	0.374	0.195	0.262	0.082		
Completed Arch Ribs (CAR)	+3°	Original	31.3	0.679	0.441	0.115		0.634	
			33.8	0.679	0.441	0.066	0.074	0.358	
		Type B	31.3	0.679	0.441	0.047	0.055	0.359	
Completed Bridge Structure (CBS)	-3°	Original	17.5	0.368		0.040		0.164	
			35.0	0.368		0.135		0.588	
		Type A	17.5	0.368		0.067		0.070	
			32.5	0.368		0.047		0.239	
		Type B	17.5	0.368		0.067		0.023	
	32.5	0.368		0.037		0.203			

Table 12: Maximum VIV amplitudes of arch ribs and corresponding wind speeds

5 CONCLUSIONS AND PROSPECTS

With the experience gained from the recently built suspension bridges, such as Akashi Kaikyo, Zhejiang Xihoumen, Great Belt, Jiangsu Runyang and Hong Kong Tsing Ma, the intrinsic limit of span length due to aerodynamic stability is about 1,500m for a traditional suspension bridge with either a streamlined box deck or a ventilative truss girder. Beyond or even approaching this limit, designers should be prepared to improve aerodynamic stability of a bridge by modifying cable system or adopting some countermeasures for girder, including vertical and/or horizontal stabilizer and slotted deck as well as passive and active control devices. Based on a preliminary study, either a widely slotted deck or a narrowly slotted deck with vertical and horizontal stabilizers could provide a 5,000m span-length suspension bridge with high enough critical wind speed, which can meet aerodynamic requirement in most typhoon-prone areas in the world.

The practice of the latest record-breaking cable-stayed bridges, Jiangsu Sutong, Hong Kong Stonecutters, Hubei Edong, Tatara and Normandy, unveils the facts that long-span cable-stayed bridges with spatial cable planes and steel box girder have high enough critical flutter speed and main aerodynamic concern in rain-wind induced vibration of long stay cables. It seems that there is still room to enlarge main span of cable-stayed bridges in the aspect of aerodynamic stability. With the development of effective solution for cable vibration mitigation, further increase or jump of span length can be expected in the near future.

The span length of arch bridges has not grown as fast as suspension bridges and cable-stayed bridges, and structural stiffness has also not reduced so much as the other two types of bridges. Based on the evidence that only one out of ten longest-span arch bridges suffered in vortex-induced problem, the enlargement of span length of arch bridges should not be influenced by aerodynamic requirement, but possibly by other aspects, for example, static instability, horizontal thrust, construction technology, and so on.

ACKNOWLEDGEMENT

The work described in this paper is partially supported by the Natural Science Foundation of China under the Grants 50538050 and 90715039, and the Hi-Tech Research and Development Program of China under the Grant 2006AA11Z108.

REFERENCES

- [1] Y.J. Ge and H.F. Xiang. Aerodynamic challenges in long-span bridges, Proceedings of Centenary Conference of the Institution of Structural Engineers, Keynote presentation, Hong Kong, China, January 24-26, 2008
- [2] Internet address A: http://en.wikipedia.org/wiki/List_of_longest_suspension_bridge_spans
- [3] A.R. Chen, Z.S. Guo, Z.Y. Zhou, R.J. Ma and D.L. Wang. Study of Aerodynamic Performance of Runyang Bridge, Technical Report WT200218, State Key Laboratory for Disaster Reduction in Civil Engineering at Tongji University (in Chinese), 2002
- [4] China Highway Planning and Design Institute. Preliminary Design Drawings of Xihoumen Bridge (in Chinese), 2003
- [5] Y.J. Ge, Y.X. Yang, F.C. Cao and L. Zhao. Study of Aerodynamic Performance and Vibration Control of Xihoumen Bridge, Technical Report WT200320, State Key Laboratory for Disaster Reduction in Civil Engineering at Tongji University (in Chinese), 2003
- [6] H.F. Xiang and Y.J. Ge. On aerodynamic limit to suspension bridges, Proceedings the 11th ICWE, Texas, USA, June 2-5, 2003
- [7] Ge Y.J. and Xiang H.F. Tomorrow's challenge in bridge span length, Proceedings of the IABSE Symposium, Budapest, Hungary, September 13-15, 2006
- [8] Ge Y.J. and Xiang H.F. Outstanding Chinese steel bridges under construction, Proceedings of the 6th International Symposium on Steel Bridges, Prague, Czech Republic, June 1-3, 2006
- [9] Y.J. Ge and H.F. Xiang. Great demand and various challenges - Chinese Major Bridges for Improving Traffic Infrastructure Nationwide, Proceedings of the IABSE Symposium, Keynote presentation, Weimar, Germany, September 19-21, 2007
- [10] Internet address B: http://en.wikipedia.org/wiki/List_of_the_largest_cable-stayed_bridges
- [11] A.R. Chen, Z.X. Lin and L.M. Sun. Testing and Study on Wind/Rain Vibration, Force Optimization and Vibration Mitigation of Stay Cables of Sutong Bridge, Technical Report WT 200419, State Key Laboratory for Disaster Reduction in Civil Engineering at Tongji University (in Chinese), 2004
- [12] H.F. Xiang, Y.J. Ge, L.D. Zhu, A.R. Chen and M. Gu. Modern Wind-Resistant Theory and Practice of Bridges. China Communications Press, Beijing, China (in Chinese), 2005
- [13] Internet address C: http://en.wikipedia.org/wiki/List_of_the_largest_arch_bridges
- [14] Shanghai Municipal Engineering Design Institute (SMEDI). Detailed Design Drawings of Shanghai Lupu Bridge (in Chinese), 2001
- [15] Y.J. Ge, F.C. Cao, J.B. Pang and Y.X. Yang. Study of Aerodynamic Performance and Wind Loading of Shanghai Lupu Bridge, Technical Report WT200103, State Key Laboratory for Disaster Reduction in Civil Engineering at Tongji University (in Chinese), 2002
- [16] Z.Y. Zhou. Numerical calculation of aeroelastic problems in bridge by random vortex method, Post-doctoral Research Report, Tongji University, China (in Chinese), 2002
- [17] Y.J. Ge and H.F. Xiang. Recent development of bridge aerodynamics in China, Proceeding of the BBAA V, Keynote presentation, Ottawa, Canada, July 20-24, 2004